



Comparison of Odin-OSIRIS OH A²Σ⁺-X²Π 0-0 mesospheric observations and ACE-FTS water vapor observations

R. L. Gattinger,¹ C. D. Boone,² K. A. Walker,² D. A. Degenstein,¹ P. F. Bernath,² and E. J. Llewellyn¹

Received 4 April 2006; revised 19 June 2006; accepted 22 June 2006; published 5 August 2006.

[1] As the production of hydroxyl (OH) in the mesosphere is driven by solar photodissociation of water vapor, the OH vertical profile is thus influenced by the water vapor profile. The details of this coupling are investigated by using experimental water vapor profiles observed by the Atmospheric Chemistry Experiment Fourier Transform Spectrometer (ACE-FTS) instrument as input to a photochemical model to predict OH profiles for comparison with experimental OH profiles observed by the Optical Spectrograph and Infra-Red Imager System (OSIRIS) instrument. We show that the model OH profiles in the 60 km to 80 km altitude region employing standard reaction rates are in agreement within 15% with the experimental OH profiles over a range of longitudes and local times, whereas the MAHRSI observations indicate the model OH densities in the middle mesosphere are approximately 30% too large. The quality of the OSIRIS OH observations and the ACE-FTS water vapor observations are both sufficiently accurate in the upper mesosphere to yield satisfactory agreement for individual profile comparisons. An example of the hemispheric maps of OH density measured by OSIRIS is shown for an altitude of 80 km. **Citation:** Gattinger, R. L., C. D. Boone, K. A. Walker, D. A. Degenstein, P. F. Bernath, and E. J. Llewellyn (2006), Comparison of Odin-OSIRIS OH A²Σ⁺-X²Π 0-0 mesospheric observations and ACE-FTS water vapor observations, *Geophys. Res. Lett.*, 33, L15808, doi:10.1029/2006GL026425.

1. Introduction

[2] There is a clear relationship between OH and water vapor [e.g., *Summers et al.*, 1997, 2001]. Further, this connection extends to ozone [e.g., *Marsh et al.*, 2003]. Global observations of OH obviously have a role to play in the study of ozone trends. The Middle Atmosphere High-Resolution Spectrograph Investigation (MAHRSI) instrument [*Conway et al.*, 1999, 2000] obtained nearly global height profiles of OH in the upper stratosphere and mesosphere during two Shuttle missions in 1994 and 1997. Their analysis included comparisons with Halogen Occultation Experiment (HALOE) [*Russell et al.*, 1993] H₂O profiles and illustrated the obvious connection to the OH profiles. *Pickett et al.* [2006] found good agreement between their

OH Microwave Limb Sounder (MLS) observations from the Aura satellite and coordinated OH observations from a balloon. Their measured MLS OH densities over the 50 km to 60 km range were systematically lower than model OH densities by 10% to 25%. *Gattinger et al.* [2006a, 2006b] (abbreviated to GDL in following text) found their OSIRIS OH observations agreed to within 15% with model OH values, based on HALOE H₂O profiles, over the 60 km to 80 km range.

[3] A coordinated analysis of mesospheric OH and H₂O profiles is presented here. Spectra of limb-scattered solar radiation from the OSIRIS instrument [*Llewellyn et al.*, 2004] on Odin [*Murtagh et al.*, 2002] are used to derive the mesospheric OH profiles. Details of the OSIRIS OH A²Σ⁺-X²Π 0-0 band analysis and OH density altitude profile generation are given by GDL. The H₂O profiles used in the photochemical model analysis are from solar occultation data obtained by the ACE-FTS instrument [*Bernath et al.*, 2005] on board SCISAT-1 provided by the Canadian Space Agency. Details of the ACE-FTS analysis and profile generation are given by *Boone et al.* [2005]. Comparisons of ACE-FTS profiles with HALOE profiles up to 75 km, including H₂O, are described by *McHugh et al.* [2005]. Due to the superior precision of the ACE-FTS water vapor measurements, validation of the accuracy in the upper mesosphere against independent data sources has not been conclusive - the estimated accuracy is 10%. In this paper we shall demonstrate the clear correlation between the OSIRIS observed OH profiles and the ACE-FTS observed H₂O profiles, particularly in the upper mesosphere.

2. Observations and Model

[4] For a number of reasons this analysis is intentionally limited to data obtained over a 24 hour period on 24 March 2005. First, both ACE-FTS and Odin-OSIRIS have nearly continuous longitude coverage on this date. Second, the pairs of individual ACE-FTS and OSIRIS observations are sufficiently close in geographic space and in time to enable valid comparisons. Finally, the ACE-FTS occultation observations at approximately 60°N latitude indicate a very pronounced longitudinal variation of H₂O mixing ratio in the upper mesosphere, and thus provide a clear test for comparison with the OSIRIS OH observations on a profile-by-profile basis.

[5] The longitudinal variation of H₂O mixing ratio as measured by the ACE-FTS instrument is shown for a single altitude of 80 km in Figure 1a. To take advantage of this significant variation for comparison with the OSIRIS OH observations, two detailed ACE-FTS profiles have been selected (Figure 1b), one at 21° West longitude (339° East

¹Institute of Space and Atmospheric Studies, Department of Physics and Engineering Physics, University of Saskatchewan, Saskatoon, Saskatchewan, Canada.

²Department of Chemistry, University of Waterloo, Waterloo, Ontario, Canada.

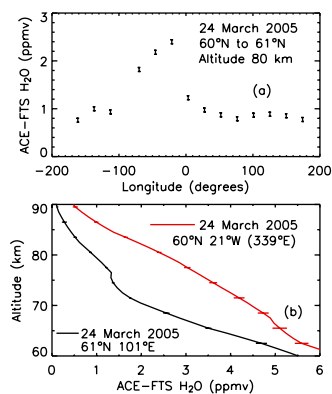


Figure 1. (a) ACE-FTS water vapor mixing ratios from 24 March 2005 for sunsets at 80 km altitude. The mixing ratio shows a very pronounced dependence on longitude. (b) Maximum and minimum ACE-FTS H₂O mixing ratio profiles used as photochemical model inputs.

longitude) near the peak of the H₂O mixing ratio and one at 101° East longitude in the region of minimum H₂O mixing ratio. Each ACE-FTS H₂O profile is obtained from a single solar occultation.

[6] The observed OSIRIS OH profile best coincident with the ACE-FTS H₂O profile in Figure 1b for maximum H₂O mixing ratio at 339° East is shown in Figure 2a, 17:25 SLT. The time difference between the OSIRIS late afternoon and the ACE-FTS sunset observations is approximately 30 minutes while the observation locations are coincident to within 300 km. The OSIRIS data for the individual profiles shown here are typically obtained in less than two minutes. The OSIRIS OH density error limits are a combination of measurement errors and calibration uncertainty (GDL).

[7] The “Model” profile in Figure 2a corresponding to the OSIRIS 17:25 SLT profile is computed with a mesospheric O_x and HO_x photochemical model (GDL) using the measured ACE-FTS maximum H₂O profile as input and with the standard reaction rates from Sander *et al.* [2003]. Temperature and density profiles are the ACE-FTS retrieved values from Version 2.2 (see Froidevaux *et al.* [2006] for comparisons with EOS MLS on the AURA satellite). Lyman α solar flux data are taken from the Solar Radiation and Climate Experiment (SORCE) database [Woods *et al.*, 2000]. Also included in Figure 2a and labeled “Rev. Chem.” is a model solution using the revised rate coefficients proposed by Summers *et al.* [1997], i.e., a 20% reduction in the O + HO₂ reaction rate together with a 30% increase in the OH + HO₂ reaction rate.

[8] To further test the comparison between OH and H₂O profiles, the OSIRIS early morning OH observations at 07:10 SLT are compared with the model for maximum H₂O mixing ratio in Figure 2a. The morning OSIRIS spatial coincidence with the nearest ACE-FTS sunset observation is 600 km and the observation times differ by approximately 11 hours. The sunrise coincidences, although still very useful, are obviously not as good as the sunset cases. The corresponding revised chemistry model solution for the early morning case is also included. The early morning model and observed OH densities in the 70 km to 85 km

range are both considerably reduced compared to the late afternoon densities shown in Figure 2a.

[9] A similar set of comparisons, but this time for minimum H₂O mixing ratio observed by ACE-FTS at 101°E (Figure 1b), is shown in Figure 2b for late afternoon OSIRIS observations at 17:25 SLT and early morning observations at 07:35 SLT. Again, the observed profiles are for individual OSIRIS limb scans and individual ACE-FTS occultations. The quality of the temporal and spatial coincidences is similar to those in Figure 2a. Again, the early morning model and observed OH densities in the 70 km to 85 km range are both considerably reduced compared to the late afternoon densities.

[10] A composite of the OSIRIS OH observations from 14 orbits on 24 March 2005 is shown as a Northern Hemisphere map for a horizontal slice at 80 km altitude in Figure 3. The data are limited to post-noon when the OH temporal variation is not nearly as pronounced as the rapid build-up in the morning hours (GDL). There are typically 7 limb scans in each daytime post-noon orbit section spanning from approximately 30°N to 80°N for a total of 90 scans in the 14 orbits. The 80 km OH density is extracted from each of the 90 profiles to assemble the map. Since the OSIRIS observations are obtained in the orbit plane, the longitudinal gaps between orbits, especially at the lower latitudes, are filled by interpolation.

3. Discussion

[11] The comparisons in Figures 2a and 2b indicate that the measured OSIRIS OH densities agree with the model OH densities to within the error limits when the standard reaction rates are used. Below 60 km the large error bars in the OSIRIS OH observations reduce the significance of the comparisons. The differences between early morning and late afternoon profiles in Figures 2a and 2b clearly show the

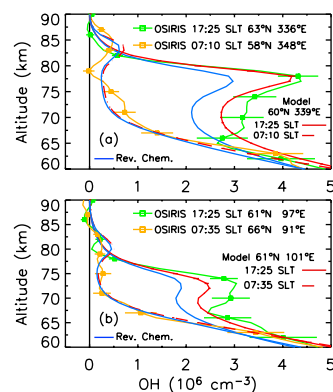


Figure 2. (a) The OSIRIS 24 March 2005 early morning and late afternoon OH profiles are compared with model OH simulations using the observed ACE-FTS maximum H₂O profile from Figure 1b. The “Rev. Chem.” model solution uses the revised reaction rates proposed by Summers *et al.* [1997] (see text for details). (b) Same as upper panel but for minimum H₂O profile from Figure 1b. The error bars are for the one-sigma level and are a combination of random measurement errors and calibration uncertainties as described by GDL.

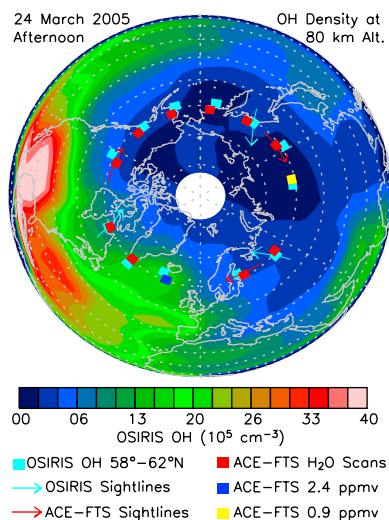


Figure 3. The 24 March 2005 post-noon OSIRIS OH Northern Hemisphere observations are assembled into a map at an altitude of 80 km. The locations of the OSIRIS limb scans in the 60°N band are shown as well as examples of the OSIRIS in-orbit viewing direction. The nearly co-located ACE-FTS H₂O occultation measurement locations are shown with the locations of maximum and minimum H₂O mixing ratios highlighted. Examples of the ACE-FTS solar occultation viewing direction are included.

strong diurnal variation of OH density in the middle and upper mesosphere. For the early morning cases the HO_x species have not had sufficient time to recover from the losses during the previous night. The recovery time in the upper mesosphere is typically several hours (GDL).

[12] The analysis of the MAHRSI OH results by *Summers et al.* [1997] indicated that models using standard reaction rates significantly over-estimate the OH density. They recommended revised reaction rates with a 20% reduction in the O + HO₂ rate together with a 30% increase in the OH + HO₂ rate. For the late afternoon cases in Figures 2a and 2b the revised chemistry model solution is clearly outside the OSIRIS OH error bar limits in the region of enhanced OH in the upper mesosphere, the region where the OSIRIS observations are most accurate. From 60 km to 65 km the case is not as clear. For the early morning observations in Figures 2a and 2b no distinction can be made between the revised chemistry and standard chemistry cases. It must be noted that the MAHRSI results are more accurate in the lower mesosphere while the OSIRIS results are more accurate in the upper mesosphere.

[13] In Figures 2a and 2b there appears to be a weak “sunrise layer” in the 80 km to 85 km region in both the observed and model OH profiles. This feature has been investigated by *Gattinger et al.* [2006b]. A similar layer was also observed at sunrise during the MAHRSI mission (Michael Stevens, private communication). A thin OH layer was also detected in the 80 km to 85 km region by LIDAR [*Hoppe et al.*, 2001].

[14] The Northern Hemisphere map of OSIRIS OH density at 80 km altitude in Figure 3 exhibits considerable variation with longitude at all latitudes and shows the

potential of these OH observations. Of specific interest for this study is the zonal variation in the 60°N region. It is apparent that the longitudinal variation of the ACE-FTS H₂O mixing ratio at 80 km altitude, 60°N latitude (Figure 1a) and the longitudinal variation of the OSIRIS OH density at 80 km altitude, 60°N latitude (Figure 3) are qualitatively very similar.

[15] A quantitative comparison is shown in Figure 4 between the OSIRIS OH density at 80 km altitude, around the 58°N to 63°N latitude band, and the model OH density using the approximately co-located ACE-FTS H₂O profiles. The observed and model OH densities are in good agreement except at densities below approximately $3 \times 10^5 \text{ cm}^{-3}$, approaching the OSIRIS detection limit in the upper mesosphere. Although the differing sightlines of OSIRIS and ACE-FTS (Figure 3) will affect the derived OH and H₂O profiles because of horizontal density variations, it is estimated the uncertainty is at least a factor of two smaller than the OH error limits included in the comparisons.

[16] The agreement between model and observed OH densities in Figure 4 suggests OSIRIS measurements can provide unique information on the upper mesospheric H₂O spatial distributions. It is important to note that the non-linear variation of OH density with H₂O density described by *Summers et al.* [2001] is clearly evident here. The model simulations for 24 March at 60°N with the prevalent low Spring H₂O mixing ratios at 80 km altitude from ACE-FTS indicate OH non-equilibrium conditions exist throughout the daylight hours resulting in considerable variation in the OH to H₂O ratio. By way of contrast, GDL (their Figure 8) show that OH equilibrium is achieved before sunset for 4 June at 62°N for a typical range of H₂O mixing ratios. Consequently, model simulations of the diurnal variation of OH are crucial to obtaining valid comparisons with H₂O densities. Also, the varying OH to H₂O ratio can produce misleading results if observations from different local times and with different H₂O mixing ratios are averaged together, particularly in the upper mesosphere where the lifetime

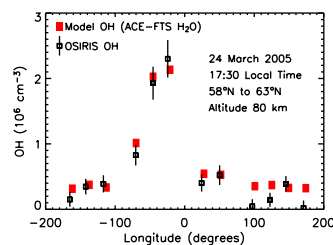


Figure 4. The OSIRIS OH densities at 80 km altitude measured in a zonal band near 60°N are compared with the model OH densities at 80 km using as model input the approximately co-located ACE-FTS H₂O profiles. Note that for the observed H₂O mixing ratios of 2.4 ppmv, and smaller, the OH density does not reach equilibrium by the end of the 12 hour day. For these non-equilibrium conditions OH is not proportional to the square root of H₂O (GDL), rather for a fixed H₂O mixing ratio the OH density can increase by a factor of three from mid-morning to mid-afternoon. For these situations the model simulations of diurnal OH variations are essential.

for Lyman α photodissociation on H_2O is of the order of one day.

4. Conclusions

[17] Comparisons between observed OSIRIS OH densities and model OH densities using observed ACE-FTS water vapor mixing ratios are shown to be in good agreement in the middle to upper mesosphere. These comparisons are valid for individual profile pairs and clearly show that longitudinal variations over a twenty-four hour period are reliably detected.

[18] We find that the adjustments to the rate constants (“Rev. Chem.”) proposed by *Summers et al.* [1997] for the lower to middle mesosphere, i.e., a 20% reduction in the $\text{O} + \text{HO}_2$ reaction rate together with a 30% increase in the $\text{OH} + \text{HO}_2$ reaction rate, are clearly not necessary in the upper mesosphere. It should be noted that since the dominant OH production source at 80 km is Lyman α while in the lower mesosphere it is $\text{O}(^1\text{D})$, this difference introduces uncertainty into the model OH profile comparisons from different missions. Nevertheless, this analysis suggests the OSIRIS OH observations can be used to infer H_2O densities in the upper mesosphere using “standard” chemistry.

[19] With this tentative validation of the OSIRIS OH product it is now possible to provide hemispheric maps of OH and H_2O density in the middle to upper mesosphere on a regular basis. With the standard OSIRIS observing schedule approximately four hemispheric maps per month can be generated.

[20] **Acknowledgments.** This work was supported by the Canadian Space Agency and the Natural Sciences and Engineering Research Council (Canada). Odin is a Swedish-led satellite project funded jointly by Sweden (SNSB), Canada (CSA), France (CNES) and Finland (Tekes). OSIRIS and ACE-FTS are supplied by the Canadian Space Agency. Support at Waterloo was also provided by the NSERC-Bomem-CSA-MSU Industrial Research Chair in Fourier Transform Spectroscopy. SORCE data are from the Laboratory for Atmospheric and Space Physics, Colorado.

References

- Bernath, P. F., et al. (2005), Atmospheric Chemistry Experiment (ACE): Mission overview, *Geophys. Res. Lett.*, *32*, L15S01, doi:10.1029/2005GL022386.
- Boone, C. D., R. Nassar, K. A. Walker, Y. Rochon, S. D. McLeod, C. P. Rinsland, and P. F. Bernath (2005), Retrievals for the atmospheric chemistry experiment Fourier-transform spectrometer, *Appl. Opt.*, *44*, 7218–7231.
- Conway, R. R., M. H. Stevens, C. M. Brown, J. G. Cardon, S. E. Zasadil, and G. H. Mount (1999), Middle Atmosphere High Resolution Spectrograph Investigation, *J. Geophys. Res.*, *104*, 16,327–16,348.
- Conway, R. R., M. E. Summers, M. H. Stevens, J. C. Cardon, P. Preusse, and D. Offermann (2000), Satellite observations of upper stratospheric and mesospheric OH: The HO_x dilemma, *Geophys. Res. Lett.*, *27*, 2613–2616.
- Froidevaux, L., et al. (2006), Early validation analyses of atmospheric profiles from EOS MLS on the Aura satellite, *IEEE Trans. Geosci. Remote Sens.*, *44*, 1106–1121.
- Gattinger, R. L., D. A. Degenstein, and E. J. Llewellyn (2006a), OSIRIS observations of mesospheric OH $\text{A}^2\Sigma^+-\text{X}^2\Pi$ 0-0 and 1-1 band resonance emissions, *J. Geophys. Res.*, *111*, D13303, doi:10.1029/2005JD006369.
- Gattinger, R. L., C. D. Boone, K. A. Walker, D. A. Degenstein, N. D. Lloyd, P. F. Bernath, and E. J. Llewellyn (2006b), OSIRIS Observations of the OH $\text{A}^2\Sigma^+-\text{X}^2\Pi$ 309 nm sunrise flash in the upper mesosphere, *Can. J. Phys.*, in press.
- Hoppe, U.-P., I. Baarstad, E. V. Thrane, T. A. Blix, R. P. Lowe, G. H. Hansen, and M. Gausa (2001), LIDAR observations of a nocturnal hydroxyl layer in the upper mesosphere at high latitudes, paper presented at XXVI General Assembly, Eur. Geophys. Soc., Nice, France.
- Llewellyn, E. J., et al. (2004), The OSIRIS Instrument on the Odin Spacecraft, *Can. J. Phys.*, *82*, 411–422.
- Marsh, D., A. Smith, and E. Noble (2003), Mesospheric ozone response to changes in water vapor, *J. Geophys. Res.*, *108*(D3), 4109, doi:10.1029/2002JD002705.
- McHugh, M., B. Magill, K. A. Walker, C. D. Boone, P. F. Bernath, and J. M. Russell III (2005), Comparison of atmospheric retrievals from ACE and HALOE, *Geophys. Res. Lett.*, *32*, L15S10, doi:10.1029/2005GL022403.
- Murtagh, D., et al. (2002), An overview of the Odin atmospheric mission, *Can. J. Phys.*, *80*, 309–319.
- Pickett, H. M., B. J. Drouin, T. Carty, L. J. Kovalenko, R. J. Salawitch, N. J. Livesey, K. W. Jucks, W. A. Traub, W. G. Read, and J. W. Waters (2006), Validation of Aura MLS HO_x measurements with remote-sensing balloon instruments, *Geophys. Res. Lett.*, *33*, L01808, doi:10.1029/2005GL024048.
- Russell, J. M., III, L. L. Gordley, J. H. Park, S. R. Drayson, D. H. Hesketh, R. J. Cicerone, A. F. Tuck, J. E. Frederick, J. E. Harries, and P. Crutzen (1993), The Halogen Occultation Experiment, *J. Geophys. Res.*, *98*(D6), 10,777–10,797.
- Sander, S. P., et al. (2003), Chemical kinetics and photochemical data for use in atmospheric studies, *JPL Publ.*, 02–25.
- Summers, M. E., R. R. Conway, R. E. Siskind, M. H. Stevens, D. Offermann, M. Riese, P. Preusse, D. F. Strobel, and J. M. Russell III (1997), Implications of satellite OH observations for middle atmospheric H_2O and ozone, *Science*, *277*, 967–970.
- Summers, M. E., R. R. Conway, C. R. Englert, D. E. Siskind, M. H. Stevens, J. M. Russell III, L. L. Gordley, and M. J. McHugh (2001), Discovery of a water vapor layer in the Arctic summer mesosphere: Implications for polar mesospheric clouds, *Geophys. Res. Lett.*, *28*, 3601–3604.
- Woods, T. N., G. J. Rottman, J. W. Harder, G. M. Lawrence, W. E. McClintock, G. A. Kopp, and C. Pankratz (2000), Overview of the EOS SORCE mission, *Proc. SPIE Int. Soc. Opt. Eng.*, *4135*, 192–203.

P. F. Bernath, C. D. Boone, and K. A. Walker, Department of Chemistry, University of Waterloo, 200 University Avenue West, Waterloo, ON, Canada N2L 3G1.

D. A. Degenstein, R. L. Gattinger, and E. J. Llewellyn, Institute of Space and Atmospheric Studies, Department of Physics and Engineering Physics, University of Saskatchewan, 116 Science Place, Saskatoon, SK, Canada S7N 5E2. (edward.llewellyn@usask.ca)